Available online at www.sciencedirect.com
SCIENCE DIRECT
Journal of Photochemistry and Photobiology A: Chemistry 180 (2006) 277–281
Journal of Photochemistry and Photobiology A:Chemistry
www.elsevier.com/locate/jphotochem

Charge-transfer as a mechanism for controlling molecular fragmentation

David Cardoza [a,*], Brett J. Pearson [a], Mark Baertschy [b], Thomas Weinacht [a,1]

[a] *Department of Physics, Stony Brook University, Stony Brook, NY 11794, USA*
[b] *Department of Physics, University of Colorado at Denver, Denver, CO 80217, USA*

Available online 10 March 2006

Abstract

We investigate control over molecular fragmentation in the halogen substituted acetone 1,1-dibromo-3,3,3-trifluoroacetone using shaped ultrafast laser pulses. Following insight gained from closed-loop learning control experiments, further tests reveal that control over the $CF_3^+/CHBr_2^+$ ratio exploits a charge-transfer mechanism. We interpret the control in terms of adiabatic rapid passage.

Keywords: Coherent control; Charge-transfer; Ultrafast spectroscopy; Wave packet dynamics

Successful implementations of closed-loop learning control over a variety of systems have helped expand the field of coherent control in recent years [1–24]. Despite the successes, control pulses are often complicated, giving little clue about the mechanism responsible for the control. While there have been a few isolated cases where the control mechanism was uncovered from optimal solutions [25–27], it remains an important goal to generalize these results and develop systematic approaches for uncovering physical insight from closed-loop control experiments [28].

In this paper, we expand on the idea of using shaped, ultrafast laser pulses as photonic reagents to investigate systematic control mechanisms within a single molecular family. This follows our previous work with a family of halogen substituted acetones including 1,1,1-trifluoroacetone (CH_3COCF_3, TFA), 1,1,1-trichloroacetone (CH_3COCCl_3, TCA), and 1,1,1-tri-deuterated acetone (CH_3COCD_3, TDA). We found that an understanding of the mechanism for controlling the CF_3^+/CH_3^+ ratio in experiments with TFA led to systematic, predictive control with other family members [27,28].

Specifically, our interpretation of the control mechanism in TFA and TCA is in terms of three basic steps: (1) ionization of the parent molecule leading to an unstable parent ion, (2) nuclear wave packet evolution on the ionic potential energy surface that leads to CX_3 (X = F, Cl) and CH_3CO^+ fragments, and (3) enhanced molecular ionization of the CX_3 fragment as the wave packet crosses through a critical C-CX_3 separation [29–33]. Here we extend the work to 1,1-3,3,3 dibromo-trifluoroacetone ($CHBr_2COCF_3$, Br_2TFA), where we find the control mechanism is based on charge transfer between separating fragments rather than enhanced molecular ionization.

1. Closed-Loop Learning Control

The details of the laser system and molecular chamber are described elsewhere [34]. Briefly, an amplified titanium:sapphire laser produces 30 fs pulses at 780 nm with maximum pulse energies of 1 mJ. An acousto-optic pulse shaper [35] interfaced with a computer shapes the laser pulses before they are focused into a molecular beam attached to an ion time-of-flight mass spectrometer (TOFMS). A genetic learning algorithm (GA) [36] searches for pulse shapes that enhance different fragmentation channels in the molecule.

As in our experiments with TCA and TFA, we used the GA to perform a global search for control over different fragment channels, unbiased toward any expected result. In the feedback experiment with Br_2TFA the GA was able to control the relative production of charged methyl fragments.

* Corresponding author. Tel.: +1 631 632 8026; fax: +1 631 632 8176.
E-mail addresses: dcardoza@stonybrook.edu (D. Cardoza), bpearson@stonybrook.edu (B.J. Pearson), mark@physics.cudenver.edu (M. Baertschy), tweinacht@stonybrook.edu (T. Weinacht)
[1] Mail address: Department of Physics, Stony Brook University, Stony Brook, NY 11794-3800, USA. Tel.: +1 631 632 8163; fax: +1 631 632 8176.

1010-6030/$ – see front matter © 2006 Elsevier B.V. All rights reserved.
doi:10.1016/j.jphotochem.2006.02.007

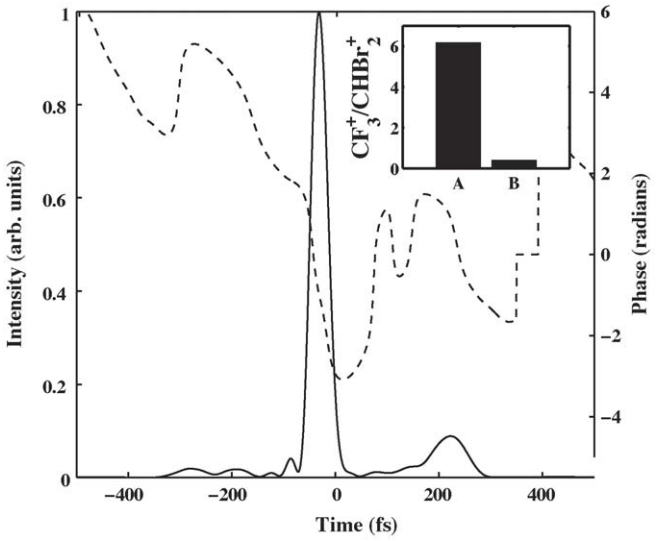

Fig. 1. Optimal control pulse for maximization of the $CF_3^+/CHBr_2^+$ ratio. The solid line denotes the intensity profile, $I(t)$, and the dashed line denotes the phase, $\phi(t)$. Inset: $CF_3^+/CHBr_2^+$ ratio when the goal was to maximize (A) the $CF_3^+/CHBr_2^+$ ratio and (B) the $CHBr_2^+/CF_3^+$ ratio.

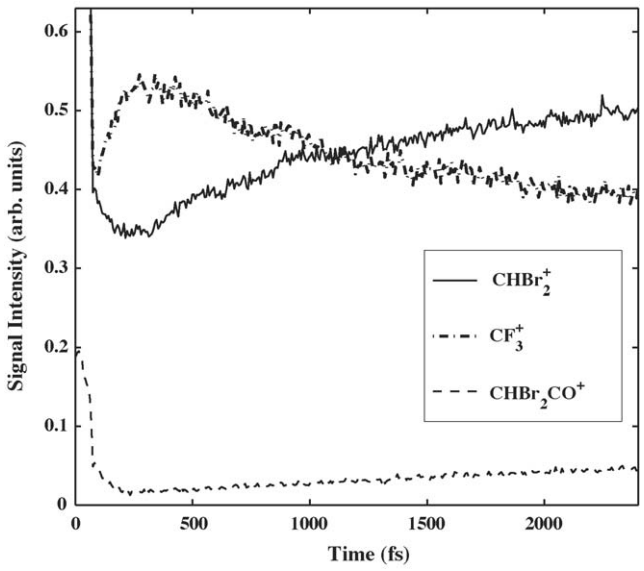

Fig. 2. $CHBr_2^+$ (solid), CF_3^+ (dash-dot) and $CHBr_2CO^+$ (dashed) signals as a function of pump-probe delay. All yields are normalized to the $CHBr_2^+$ signal at zero time delay.

Fig. 1 shows the temporal phase and intensity for an optimal laser pulse when maximizing the ratio of $CF_3^+/CHBr_2^+$. The pulse has a high intensity ($\sim 1 \times 10^{14}$ W/cm^2), nearly transform-limited primary pulse, followed by a less intense, longer pulse approximately 300 fs later. Repeated runs of the GA produced similar solutions, with the time delay between the two pulses varying from 250 to 300 fs. The optimal pulse for maximizing the ratio of $CHBr_2^+/CF_3^+$ is a low intensity unshaped pulse. The inset to Fig. 1 shows the control ratio achieved when maximizing the production of either CF_3^+ (A) or $CHBr_2^+$ (B).

Although the control experiments with Br_2TFA were similar to those with TFA and TCA, subtle differences in the results suggest a different underlying control mechanism. For TFA and TCA the optimal pulses were composed of a series of pulses with the two main sub-pulses having similar intensity. For Br_2TFA, an intense pulse is followed by a substantially less intense pulse, which would be relatively ineffective for enhanced ionization. Additionally, the control in Br_2TFA was more pronounced than in TFA or TCA (over an order of magnitude in the fragment ratio for Br_2TFA), largely because of the more substantial decrease in the $CHBr_2^+$ yield (compared with CH_3^+) for an optimal pulse. Finally, rough estimates of fragment kinetic energies (achieved by measuring the dependence of the control on laser polarization [27]) indicate that the CF_3^+ fragments in Br_2TFA acquire no additional kinetic energy with an optimal pulse. In the TFA experiments using the optimal pulse shape substantially increased the kinetic energy of the CF_3^+ fragments.

2. Pump-probe spectroscopy

As with TFA and TCA, the optimal pulse structure suggests that fragment dynamics play a role in the control mechanism. We investigated this further with a series of pump-probe experiments to measure fragment yields as a function of time delay between the two laser pulses. In these experiments the intensity of the probe pulse was about a factor of four less than that of the pump pulse so that it was incapable of photoionizing any of the molecules.

The yields for CF_3^+, $CHBr_2^+$, and $CHBr_2CO^+$ are shown in Fig. 2. Production of CF_3^+ is maximized at a delay of $\sim$ 300 fs. Coinciding with this is a decrease in the $CHBr_2^+$ signal. The $CHBr_2CO^+$ signal also appears to be anti-correlated with the CF_3^+ signal except for small delays when the overlapping pulses produce an anomalously large ion signal. The depths of modulation are significant, approaching 25% of the ($t \rightarrow \infty$) asymptotic values. Also, we note that the sum of the three ion signals is roughly constant.

The peak in the CF_3^+ yield is similar to results with TFA and TCA. However, the accompanying decrease in the $CHBr_2CO^+$ and $CHBr_2^+$ signals is different (with TFA and TCA the CH_3^+ fragment showed no modulation) and suggests that charge is transferred from CF_3 to either $CHBr_2CO^+$ or $CHBr_2^+$ [37]. Furthermore, with charge-transfer, as opposed to enhanced ionization, the absence of a coulomb repulsion between two closely spaced, charged fragments explains the lack of energetic fragments during control. Before describing further tests of this charge transfer model, we will discuss formation of the fragments from the parent molecule.

3. Fragmentation pathways

In the experiments with TFA or TCA, ionization on the leading edge of the laser pulse produced CF_3 (or CCl_3) and CH_3CO^+ because of the instability of the parent ions. As there is no significant $CHBr_2COCF_3^+$ in the TOFMS for Br_2TFA, we infer that $CHBr_2COCF_3^+$ also auto-dissociates. However, unlike TFA and TCA, the fragmentation of $CHBr_2COCF_3^+$ is not dominated by a single dissociation channel (such as for-

mation of CH_3CO^+ and CF_3 in TFA). $CHBr_2^+$ production is significant at all intensities, so we must consider at least two dissociation channels for the parent ion leading to final products $CHBr_2CO^+ + CF_3$ or $CHBr_2^+ + CO + CF_3$. While not critical for the analysis below, we hypothesize that these final products are formed first by dissociation of $CHBr_2COCF_3^+$ into $CHBr_2CO^+$ and CF_3^+, and then possibly further dissociation of $CHBr_2CO^+$ into $CHBr_2^+$ and CO. This hypothesis is based upon several observations. One is that ionization removes an electron from an orbital on the CO, and another is that CF_3CO^+ is relatively unstable and not produced in our experiment. Finally, the $CHBr_2^+$ and $CHBr_2CO^+$ yields are correlated, and have similar dependence on laser intensity as discussed below.

In order to better understand the fragmentation following ionization, we measured the fragment yields as a function of intensity for a single, transform-limited laser pulse. The yields for $CHBr_2CO^+$, $CHBr_2^+$, and CF_3^+ as a function of peak intensity are shown on a log–log scale in Fig. 3. The FWHM of the pulse was kept at a constant 35 fs. On a log–log scale the $CHBr_2^+$ and $CHBr_2CO^+$ yields as a function of pulse intensity have slopes of 3.5 and 3.2, respectively. This indicates that $CHBr_2^+$ and $CHBr_2CO^+$ are produced by processes of similar multi-photon order. However, the CF_3^+ yield has a slope of 4.4 indicating that production of CF_3^+ is a higher order process.

At low laser intensities the parent ion dissociates primarily into $CHBr_2CO^+$ and neutral CF_3. If the $CHBr_2CO^+$ fragment is left in an excited state it then dissociates into $CHBr_2^+$ and CO with the branching ratio for this three-way fragmentation channel increasing slightly with pulse intensity. Therefore, ionization of Br_2TFA can launch a wave packet on two different, but energetically close, potential energy surfaces (PES's) corresponding to the two dissociation channels $CHBr_2CO^+ + CF_3$ and $CHBr_2CO^{+*} + CF_3 \rightarrow CHBr_2^+ + CO + CF_3$.

4. Dynamic Resonance

Because the changes in fragment yields are relatively large and appear to show a high degree of anti-correlation, we believe that the PES leading to CF_3^+ and the PES's leading to $CHBr_2CO^+$ and $CHBr_2^+$ must be strongly coupled by the probe pulse. The strong coupling of these surfaces by the laser pulse suggests that the coupling is resonance mediated and the time dependence of the coupling suggests that the resonance is dynamic [38]. These observations lead to the hypothesis that the charge-transfer is mediated by adiabatic rapid passage (ARP)—with a twist. In the usual form of ARP [39], the laser frequency is adiabatically swept, or "chirped", through a static atomic or molecular resonance. For this dynamic ARP, the laser frequency can remain fixed while the difference in energy between two molecular electronic states sweeps through a resonance.

Fig. 4 shows the hypothetical PES's that describe the dynamics associated with the control mechanism. The pump pulse launches a wave packet from the neutral ground state of the molecule (PES 1) onto a dissociative ionic PES (PES 2) representing fragmentation into $CHBr_2CO^{+*} + CF_3$ or $CHBr_2CO^+ + CF_3$. When the probe pulse comes $\sim$ 350 fs later, the wave packet is promoted to another dissociative ionic PES (PES 3) that leads to $CHBr_2CO + CF_3^+$.

In a dressed state picture of the molecular levels, the two electronic states associated with PES's 2 and 3 in Fig. 4 are made degenerate by the laser but, because of their coupling, there is an avoided crossing. Depending on the electric field strength of the laser and the speed of the fragments, the avoided crossing can be traversed diabatically, resulting in little population transfer between the states, or adiabatically, resulting in almost full transfer. We now describe the results of several tests of the dynamic ARP hypothesis.

Our first test was to measure how the charge-transfer depends on probe pulse intensity. Fig. 5 shows the ion signals as a function of probe intensity, with the probe pulse coming 350 fs after a

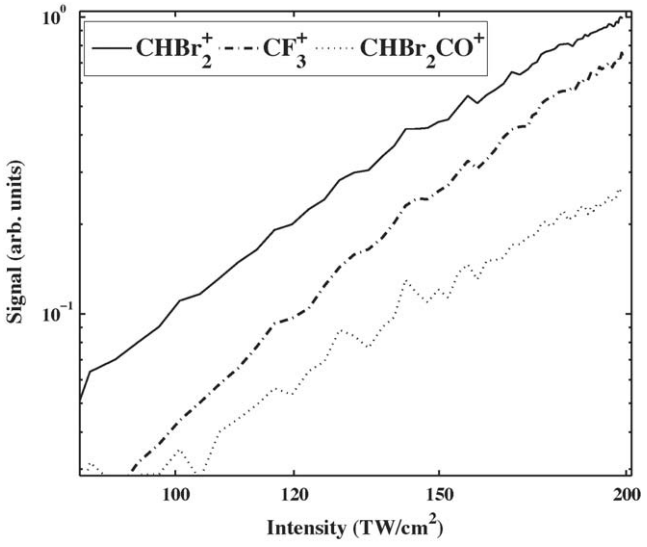

Fig. 3. $CHBr_2^+$ (solid), CF_3^+ (dashed-dot) and $CHBr_2CO^+$ (dotted) signals as a function of pulse peak intensity plotted on a log–log scale.

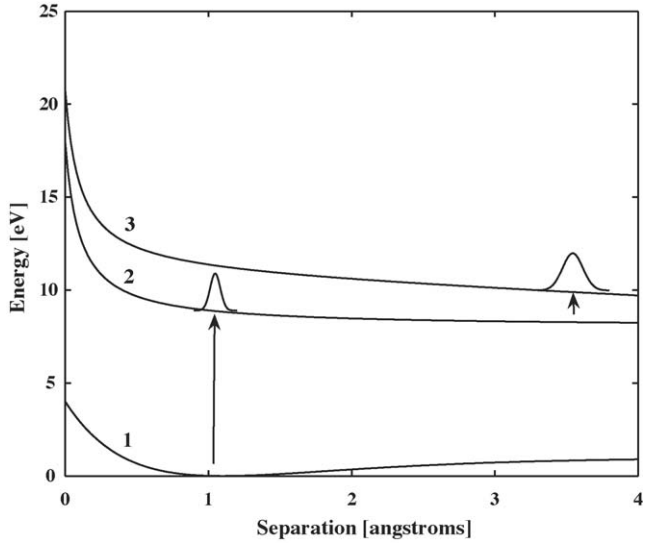

Fig. 4. Simplified cartoon of hypothetical potential energy surfaces involved in the control mechanism.

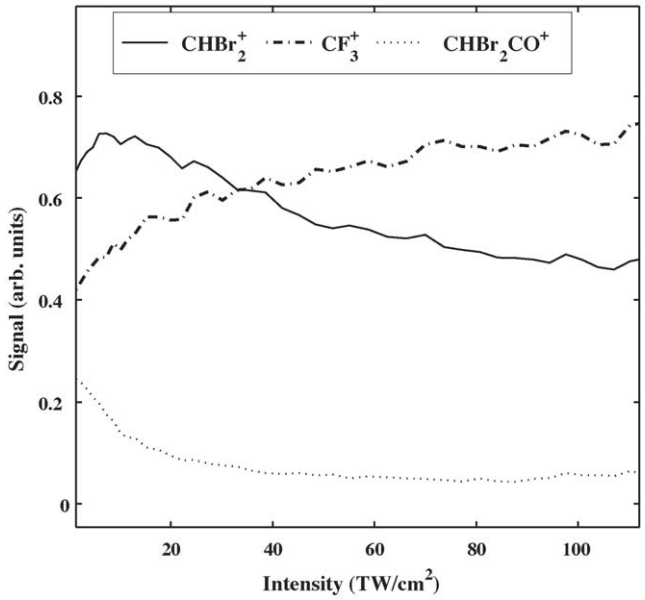

Fig. 5. $CHBr_2^+$ (solid), CF_3^+ (dashed) and $CHBr_2CO^+$ (dotted) signals as a function of peak intensity, for a fixed pulse duration. This data was taken while scanning the intensity of the probe pulse, which was timed to coincide with the CF_3^+ enhancements seen in Fig. 2.

transform limited pump pulse. The CF_3^+ signal increases rapidly for low intensities but saturates at higher intensities, as expected for ARP [39]. Increasing the Rabi frequency, e.g., by increasing pulse intensity, allows one to change the passage from diabatic to adiabatic. Once the Rabi frequency becomes large enough to satisfy the adiabatic condition [39], there is no further increase in population transfer.

The intensity dependences seen in Fig. 5 are distinctly different from those of the single pulse intensity scan shown in Fig. 3. When the probe pulse energy is increased, production of $CHBr_2CO^+$ and $CHBr_2^+$ actually decreases (aside from a small initial increase in $CHBr_2^+$) and is anti-correlated with the CF_3^+ fragment. Furthermore, the combined decrease in $CHBr_2CO^+$ and $CHBr_2^+$ yields is equivalent to the increase in CF_3^+ yield – the sum of the three varies by less than 3%.

The ARP charge transfer model is supported by both the learning control and the pump-probe data but has not yet explained the widths of the peaks in the pump-probe data. Our first hypothesis was that the widths correspond to the time during which the PES's are resonantly coupled by the laser pulse. To test this, we repeated the pump-probe measurements (see Fig. 2) with two different central frequencies (380 and 391 THz) for the probe pulse while limiting its bandwidth enough to nearly double its duration. Peak timings or widths for the $CHBr_2^+$ and CF_3^+ fragment yields in these two scans were similar to each other and to earlier pump-probe results with the full laser bandwidth. There were slight differences in the $CHBr_2CO^+$ peak, but these are difficult to analyze because of the long duration of this peak. Since analysis of the $CHBr_2CO^+$ fragment dynamics is not central to this paper, we leave that for a future discussion.

Based on the $CHBr_2^+$ and CF_3^+ behavior we conclude that the widths of the pump-probe peaks are not limited by the laser

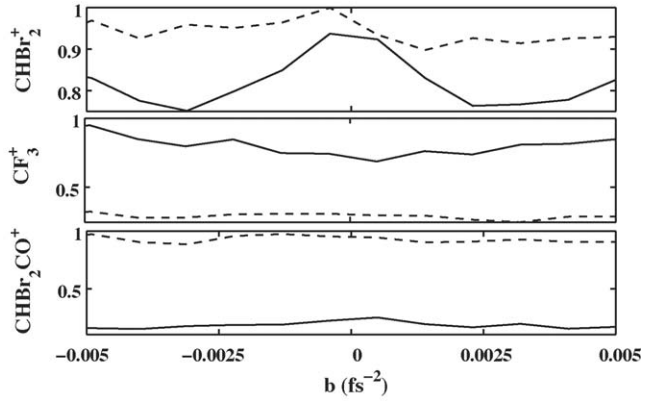

Fig. 6. $CHBr_2^+$, CF_3^+, and $CHBr_2CO^+$ yields as a function of chirp parameter b where the temporal phase of the probe pulse, with central frequency ω_0, is $\phi(t) = \omega_0 t + bt^2$. Data are shown for the maximum probe pulse intensity (solid) and for lower intensity (dashed).

bandwidth. Instead, they must be dictated by the spread of the dissociating wave packet as it crosses the resonance. Hence, the pump-probe data represents a measurement of the quantum mechanical probability density of the wave packet. Furthermore, the fact that the pump-probe peaks did not move by more than 50 fs with probe pulse tuning places a lower limit on the molecular chirp rate of ~210 THz/ps.

If the spread of the wave function of the dissociating molecule does determine the width of the peaks in the pump-probe data, then increasing the duration of the probe pulse (to better match wave function spread) should increase the charge-transfer — as long as the probe pulse has sufficient intensity to strongly couple the PES's and make the transition across the resonance adiabatic. To test this, we measured fragment yields as a function of probe pulse duration for two different probe energies.

Fig. 6 shows the CF_3^+, $CHBr_2^+$, and $CHBr_2CO^+$ signals as a function of second-order spectral phase ("chirp"). Probe pulse duration is related to the chirp parameter, b, by

$$\tau = \frac{2\ln(2)}{\pi\Delta\nu}\sqrt{1+\frac{b^2}{a^2}},$$

where $\Delta\nu$ is the laser bandwidth (15.8 THz), and $a = ln2/\tau_p^2$ (8.8×10^{-4} fs^{-2}) where τ_p is the transform limited pulse duration (28 fs). By adjusting the chirp to change the probe pulse duration we kept the probe pulse energy fixed and confirmed our lower bound for the molecular chirp rate by comparing the charge-transfer with positive and negative laser chirp. The pump-probe time delay was set to 280 fs (roughly the peak of the charge-transfer process) and chirp rate was kept below 80 THz/ps to avoid overlap of the stretched probe pulse with the pump.

For a low probe energy (~ 50 μJ), there is little variation in the fragment yields as a function of probe pulse duration. However, for a higher probe energy (~ 100 μJ), the $CHBr_2^+$ and $CHBr_2CO^+$ ion signals go down with increasing probe pulse duration, while the CF_3^+ signal *increases* with increasing probe pulse duration. This is consistent with the pump-probe signal width being limited by the spread of the dissociative wave func-

tion. Only the portion of the wave function in the vicinity of the resonance *while the probe pulse is on* can be transferred between PES's.

Furthermore, while there is a slight asymmetry in the data with respect to positive and negative laser chirp, the lack of a substantial difference means that the molecular chirp rate must be much larger than the maximum probe laser chirp rate of 80 THz/ps. This is consistent with our earlier lower bound of 210 THz/ps. The slight asymmetry is consistent with the positive chirp making the passage more diabatic while the negative chirp makes the passage more adiabatic. A laser frequency sweep in the same direction of the molecular chirp should make the process further adiabatic, thereby enhancing charge-transfer.

5. Conclusions and future directions

We have extended learning control in the halogenated acetones to Br_2TFA and uncovered a control mechanism based on charge-transfer through adiabatic rapid passage. This charge-transfer mechanism involves both nuclear and electronic coherences, demonstrating that it is possible to exploit coherence between different electronic states for control and to understand such control. This control mechanism also opens the possibility of directly measuring the molecular wave function during dissociation [40,41]. The pump-probe data represents a measurement of the probability density of the molecular wave function on the lower PES and is not limited by the probe pulse bandwidth or duration. Our current experiment gives a rough measure of the wave function amplitude, but simple extensions involving the interference of two wave packets could yield the phase as well.

Acknowledgements

This research used resources of the National Energy Research Scientific Computing Center, which is supported by the Office of Science of the U.S. Department of Energy under Contract No. DE-AC03-76SF00098. This research is supported by the National Science Foundation under award number 0244748. We acknowledge the donors to the American Chemical Society Petroleum Research Fund for partial support of this research.

References

[1] R. Judson, H. Rabitz, Phys. Rev. Lett. 68 (1992) 1500.
[2] P. Brumer, M. Shapiro, Chem. Phys. Lett. 126 (6) (1986) 541–546.
[3] D. Tannor, S. Rice, J. Chem. Phys. 83 (1985) 5013.
[4] C. Bardeen, V. Yakovlev, K. Wilson, S. Carpenter, P. Weber, W. Warren, Chem. Phys. Lett. 280 (1997) 151.
[5] R. Levis, G. Menkir, H. Rabitz, Science 292 (2001) 709.
[6] L. Zhu, V. Kleiman, X. Li, S. Lu, K. Trentelman, R. Gordon, Science 270 (1995) 77.
[7] T. Witte, T. Hornung, L. Windhorn, R. deVivie Riedle, D. Proch, M. Motzkus, K. Kompa, J. Chem. Phys. 118 (2003) 2021–2024.
[8] J. Herek, W. Wohlleben, R. Cogdell, D. Zeidler, M. Motzkus, Nature 417 (2002) 533.
[9] T. Weinacht, J. Ahn, P. Bucksbaum, Nature 397 (1999) 233.
[10] R. Minns, J. Verlet, L. Watkins, H. Fielding, J. Chem. Phys. 119 (2003) 5842.
[11] R. Bartels, S. Backus, E. Zeek, L. Misoguti, G. Vdovin, I. Christov, M. Murnane, H. Kapteyn, Nature 406 (2000) 164.
[12] A. Flettner, J. Günther, M. Mason, U. Weichmann, R. Düren, G. Gerber, App. Phys. B 73 (2001) 129.
[13] H. Ohmura, T. Nakanaga, M. Tachiya, Phys. Rev. Lett. 92 (2004) 113002.
[14] D. Meshulach, Y. Silberberg, Nature 396 (1998) 239.
[15] T. Brixner, N. Damrauer, G. Krampert, P. Niklaus, G. Gerber, J. Mod. Opt. 50 (2003) 539.
[16] N. Damrauer, C. Dietl, G. Krampert, S.-H. Lee, K.-H. Jung, G. Gerber, Eur. Phys. J. D 20 (2002) 71.
[17] Z. Amitay, J. Ballard, H. Stauffer, S. Leone, Chem. Phys. 267 (2001) 141.
[18] Š. Vajda, A. Bartelt, E.-C. Kaposta, T. Leisner, C. Lupulescu, S. Minemoto, P. Rosendo-Francisco, L. Wöste, Chem. Phys. 267 (2001) 231.
[19] M. Dantus, Annu. Rev. Phys. Chem. 52 (2001) 639.
[20] A. Lindinger, C. Lupulescu, M. Plewicki, F. Vetter, A. Merli, S. Weber, L. Wöste, Phys. Rev. Lett. 93 (2004) 033001.
[21] T.C. Weinacht, R.A. Bartels, S. Backus, B. Pearson, P.H. Bucksbaum, J. Geremia, H. Rabitz, H.C. Kapteyn, M.M. Murnane, Chem. Phys. Lett. 344 (2001) 333.
[22] B.J. Pearson, P.H. Bucksbaum, Phys. Rev. Lett. 92 (2004) 243003.
[23] T.C. Weinacht, J.L. White, P.H. Bucksbaum, J. Phys. Chem. A 103 (1999) 10166–10168.
[24] J. Konradi, A.K. Singh, A. Materny, Phys. Chem. Chem. Phys 7 (2005) 3574–3579.
[25] C. Daniel, J. Full, L. González, C. Lupulescu, J. Manz, A. Merli, Š. Vajda, L. Wöste, Science 299 (2003) 536.
[26] R. Bartels, M. Murnane, H. Kapteyn, I. Christov, H. Rabitz, Phys. Rev. A. 70 (2004) 043404.
[27] D. Cardoza, M. Baertschy, T.C. Weinacht, J. Chem. Phys. 123 (2005) 074315.
[28] D. Cardoza, M. Baertschy, T.C. Weinacht, Chem. Phys. Lett. 411 (2005) 311.
[29] M. Ivanov, T. Seideman, P. Corkum, P. Dietrich, F. Ilkov, Phys. Rev. A 54 (1996) 1541.
[30] D.M. Villeneuve, M.Y. Ivanov, P.B. Corkum, Phys. Rev. A 54 (1996) 736.
[31] T. Zhou, S. Chelkowski, A.D. Bandrauk, Phys. Rev. A 48 (1993) 3837.
[32] T. Seideman, M.Y. Ivanov, P.B. Corkum, Chem. Phys. Lett. 252 (1996) 181.
[33] S. Menon, J.P. Nibarger, G.N. Gibson, J. Phys. B. 35 (2002) 2961.
[34] F. Langhojer, D. Cardoza, M. Baertschy, T. Weinacht, J. Chem. Phys. 122 (2005) 01402.
[35] M.A. Dugan, J.X. Tull, W.S. Warren, J. Opt. Soc. Am. B 14 (1997) 2348.
[36] L. Davis, A Handbook of Genetic Algorithms, van Nostrand Reinhold, 1991.
[37] S.A. Trushin, W. Fuss, W.E. Schmid, J. Phys. B. 37 (2004) 3987.
[38] S. Gräfe, V. Engel, Chem. Phys. Lett. 414 (2005) 17–22.
[39] D. Goswami, Physics Reports 374 (2003) 385.
[40] S. Gräfe, D. Scheidel, V. Engel, N.E. Henriksen, K.B. Møller, J. Phys. Chem. A 108 (2004) 8954–8960.
[41] J. Degert, C. Meier, B. Chatel, B. Girard, Phys. Rev. A (2003) 041402(R).